Supporting Information

Marquardt, I., Schneider, M., Gulban, O. F., Ivanov, D., & Uludag, K. (2018). Cortical depth profiles of luminance contrast responses in human V1 and V2 using 7T fMRI. *Human Brain Mapping*. https://doi.org/10.1002/hbm.24042

Spatial resolution & upsampling

At the currently achievable spatial resolution of fMRI, each voxel typically covers more than one cortical layer. Therefore, it is necessary for laminar fMRI studies to increase the effective spatial resolution via post-processing. This can be achieved by upsampling (as in the present study), or by another super-resolution approach, such as spatial GLM ("unmixing") [Kok et al., 2016]. Either of these approaches is based on two assumptions: a) the activity of each layer is similar across cortical locations within the ROI investigated, and b) the voxels included in the ROI sufficiently sample the layers with different spatial weights (i.e. the voxels differ in the partial volume contributions from the layers). The rationale behind upsampling or unmixing can be compared to the increase in effective temporal resolution achieved by jittering in event related designs, where a) would correspond to the assumption of a similar response across trials, and b) would be analogous to sampling enough trials at different (jittered) time points. To the best of our knowledge, assumption a) is common to all cortical depth specific fMRI studies but in principle requires validation for each stimulus type and ROI investigated. We think that for a simple contrast stimulus, as used in the current study, assumption a) is very likely to be true in V1 and V2. Assumption b) requires a minimum spatial extent of the ROI and quasi-random location of the voxels relative to the cortical layers, which should be fulfilled given the spatial dimensions and curvature of the V1 and V2 ROIs.

Given the need to upsample and interpolate, we tried to minimise its effect on our statistical results. To this end, we performed the GLM analysis on the original time series data

in volume space, without upsampling, and with no interpolation except for motion correction and distortion correction. For the sole purpose of more fine-grained tissue type segmentations, we upsampled the T1 images using trilinear interpolation. The slight blurring introduced by trilinear interpolation is, in our experience, beneficial for anatomically plausible tissue type segmentation. In contrast to common practice in most low-resolution fMRI studies, it was the anatomical T1 images, which were registered to the mean functional EPI image, thus avoiding the need to interpolate the statistical maps at this step. The mean functional EPI images and the statistical maps were upsampled to the same resolution as the T1 images and corresponding tissue type segmentations using nearest-neighbour interpolation. Please note that the upsampling of the mean functional EPI images and of the statistical maps was only performed for practical reasons (without this step, the mean EPI images and the statistical maps would have been at a different resolution than and the fine-grained tissue type segmentations, which would have complicated the analysis pipeline). The actual increase in effective spatial resolution is obtained during the subsequent cortical depth sampling. Cortical depth sampling was performed using nearest-neighbour interpolation, but we did not find a linear interpolation algorithm to produce significantly different results.

Alternatively, one may perform cortical depth-sampling directly on the fMRI time series data, and perform GLM fitting on time courses averaged across the region of interest, separately at each depth level. However, the ROIs within which the depth-sampling was performed were selected based on the results of the GLM, in order to sample from regions of cortex that actually respond to the stimulus (see Figure 2 in the main text). Thus, in our approach, the depth sampling necessarily has to be performed after the GLM fitting. Under the assumption of spatially homogeneous noise (within the ROI), no differences between the two alternative approaches are expected (i.e. GLM fitting on average ROI time courses, or averaging GLM parameter estimates within the ROI).

Supplementary Figures

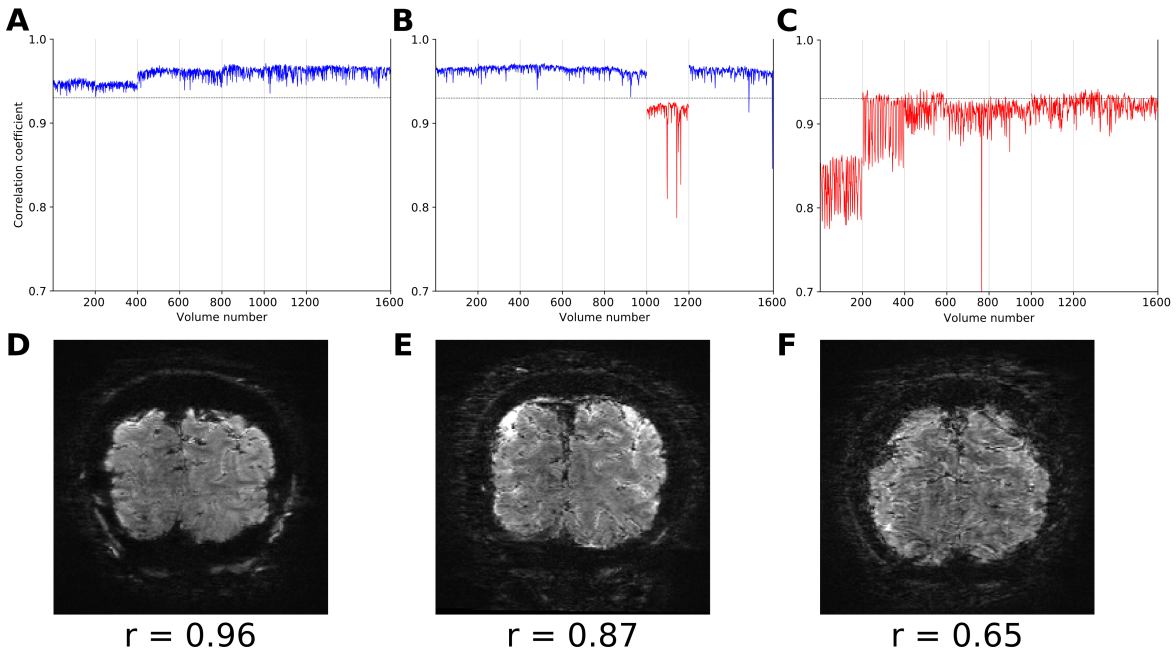

Supplementary Figure S1. Quality control. In order to remove data affected by artefacts based on a quantitative criterion, the correlation of the voxel intensity between each EPI volume and the mean EPI image of the respective session was calculated. (A, B, C) Spatial correlation over time for three subjects. Runs with a mean correlation coefficient below criterion ($r < 0.93$) are plotted in red. The threshold was chosen to differentiate between data with a high and stable correlation (A), and runs with a low and unstable correlation (e.g. the second-last run in B, and all runs in C). Upon visual inspection, runs with a low correlation coefficient showed geometric distortions, ringing artefacts and intensity fluctuations, presumably due to subject head motion or physiological artefacts. (A) For this subject, no runs were excluded. (B) Only the second-last run was excluded for this subject. (C) All runs are below criterion, thus the entire session was excluded from analysis. (D, E, F) Example EPI slices illustrating the correspondence between image quality and spatial correlation. The images are taken from the subjects shown in A, B, and C, respectively. The lower data quality (i.e. distortions, ringing and blurring) in E, and especially in F, compared to D is reflected in a lower spatial correlation coefficient.

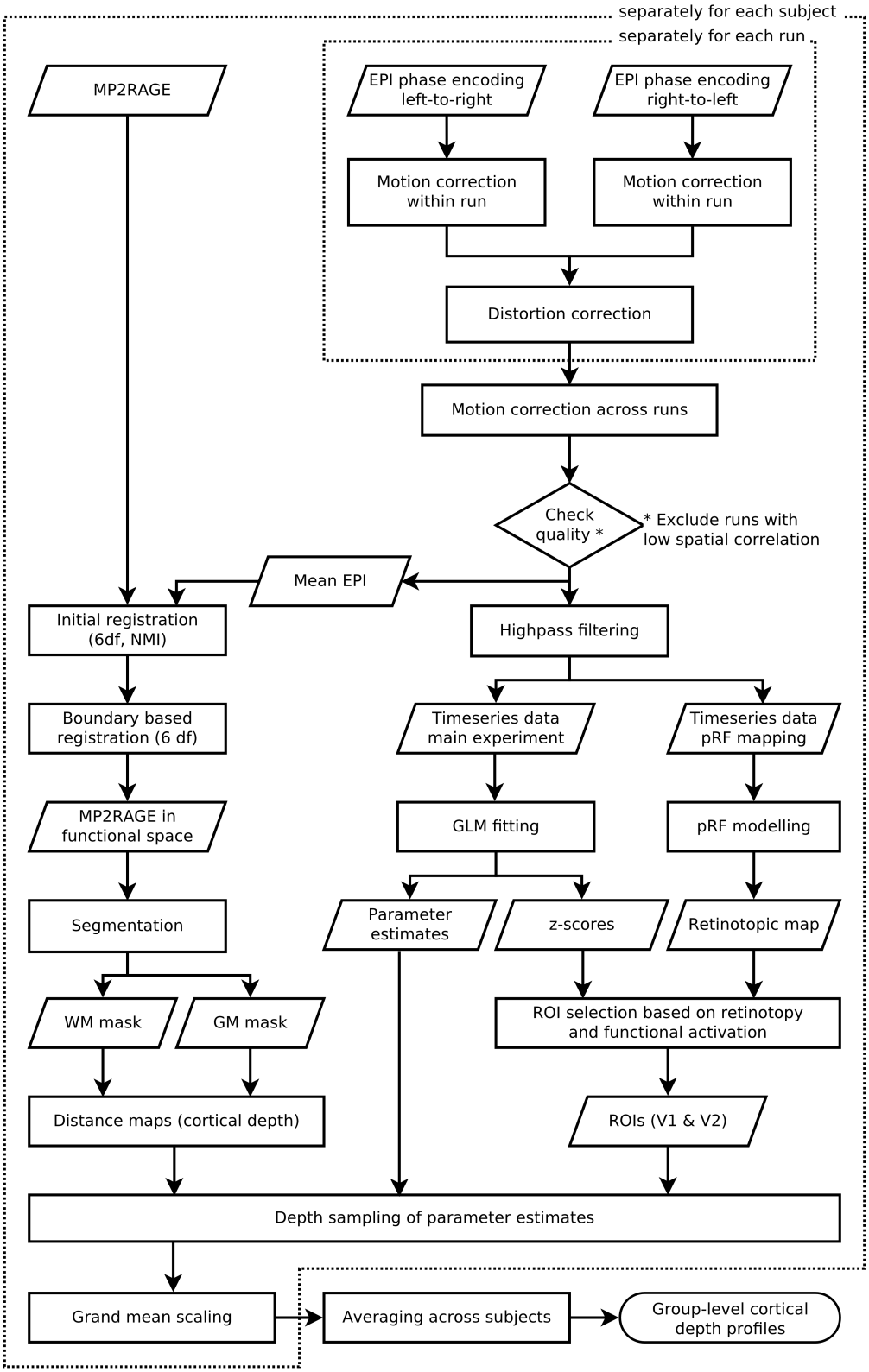

Supplementary Figure S2. Details of the preprocessing & analysis pipeline.

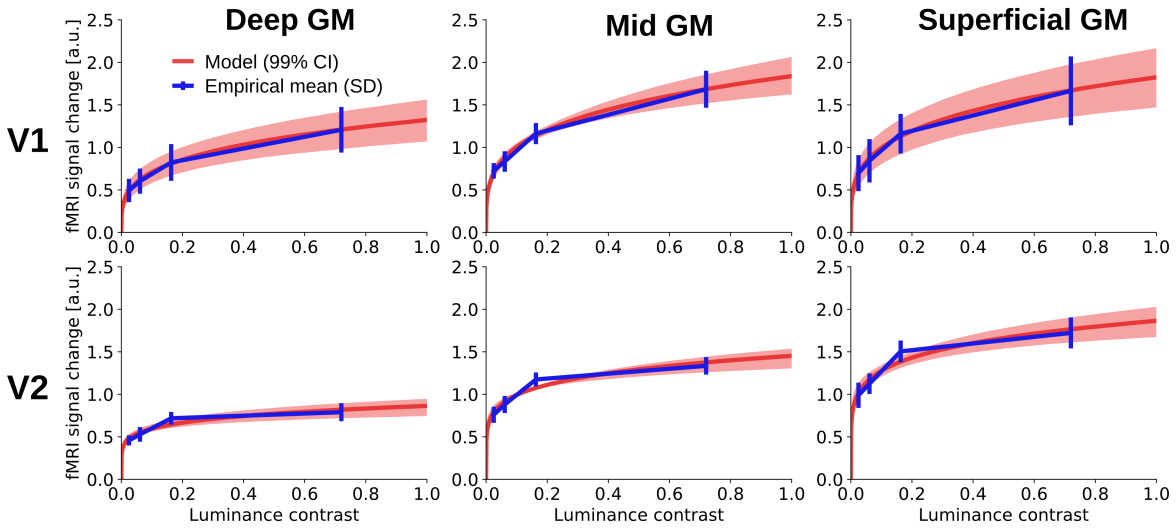

Supplementary Figure S3. Same as Figure 5 in the main text, but before spatial deconvolution.

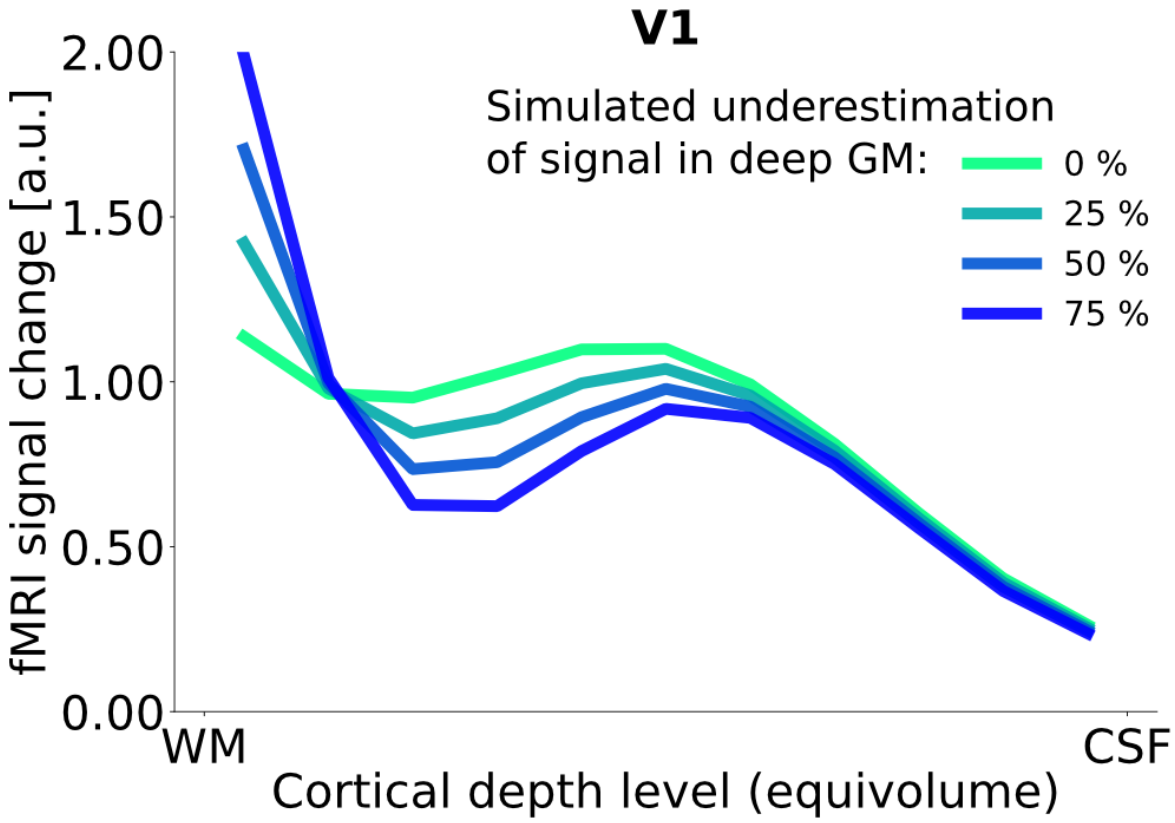

Supplementary Figure S4. Simulation of an underestimation of the response amplitude at the deepest cortical depth level due to partial volume effects at the white matter/grey matter boundary. Although we have taken great care to not include white matter voxels in the grey matter segmentation, residual errors and partial volume effects may be present. Because white matter voxels are not expected to show a response to the visual stimulus, partial voluming with adjacent grey matter could result in an underestimation of the response amplitude in the deep grey matter. Here, we simulated the effect of underestimating the signal at the deepest cortical depth level (closest to white matter) by 25%, 50%, and 75%. The stimulus-induced response amplitude at the deepest cortical depth level was multiplied by the respective scaling factor (e.g. 1.25 for a 25% underestimation), to produce the hypothetical true response amplitude for each scenario, and the deconvolution was applied. The line labelled 0% corresponds to the depth profile in the main manuscript (same as Figure 4B). For better visibility, data are only plotted for one stimulus condition (72% luminance contrast). The general shape of the profile (i.e. presence of deep grey matter and mid grey matter peaks) is not affected. However, in case of an underestimated deep grey matter response, the mid grey matter peak is more pronounced, at a slightly lower amplitude.

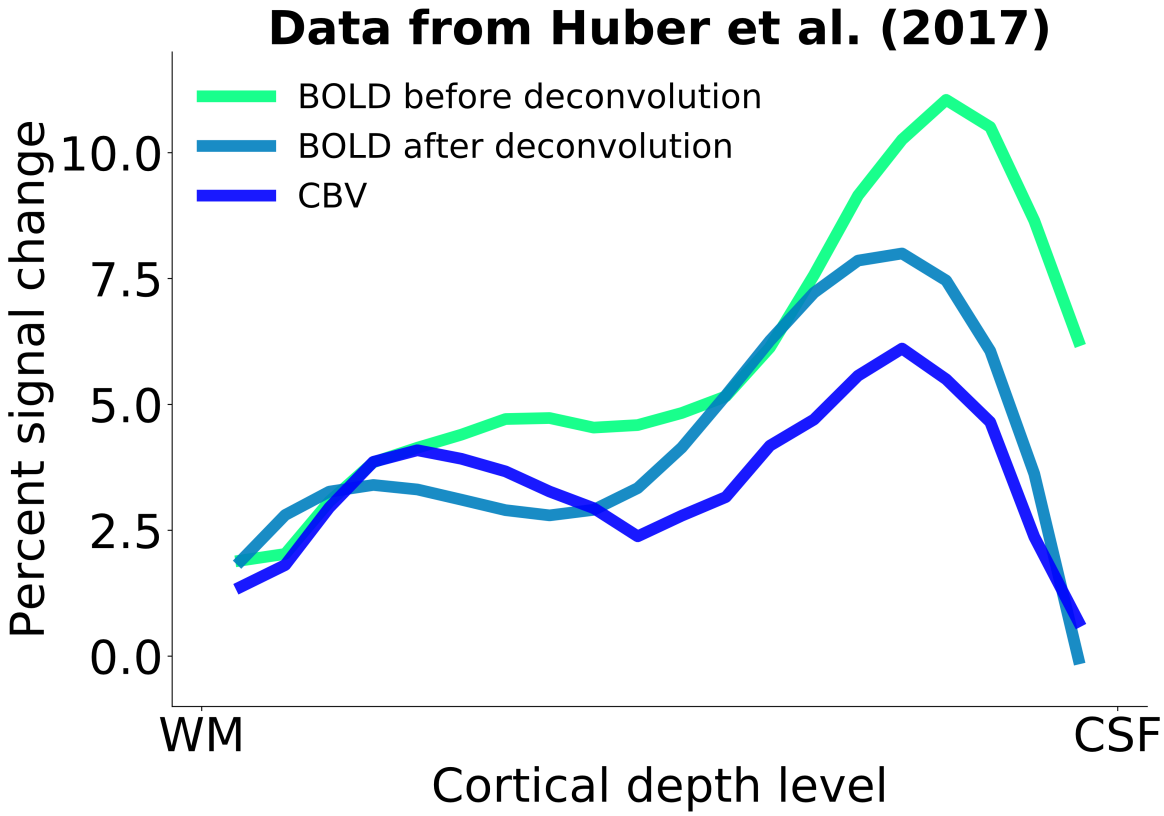

Supplementary Figure S5. Spatial deconvolution applied to BOLD fMRI cortical depth profiles of task-induced activity in primary motor cortex (M1), and profile of cortical blood volume (CBV), from Huber et al. [2017a]. CBV was measured using the VASO sequence. Because CBV changes are thought to stem mostly from the microvasculature [see Uludag and Blinder, 2017 for a review], the CBV profile is expected to more closely reflect underlying local neuronal activity. Even though the deconvolution model is not optimised for M1, the deconvolution brings the BOLD signal closer to the CBV profile.

References

Kok, P., Bains, L. J., vanMourik, T., Norris, D. G., & deLange, F. P. (2016). Selective Activation of the Deep Layers of the Human Primary Visual Cortex by Top-Down Feedback. *Current Biology*, 26(3), 371376. https://doi.org/10.1016/j.cub.2015.12.038

Huber, L., Handwerker, D. A., Jangraw, D. C., Chen, G., Hall, A., Stber, C., ... Bandettini, P. A. (2017a). High-Resolution CBV-fMRI Allows Mapping of Laminar Activity and Connectivity of Cortical Input and Output in Human M1. *Neuron*. https://doi.org/10.1016/j.neuron.2017.11.005

Uludag, K., & Blinder, P. (2017). Linking brain vascular physiology to hemodynamic response in ultra-high field MRI. *NeuroImage*. https://doi.org/10.1016/j.neuroimage.2017.02.063